Summer 8-2023

Ultrasensitive Tapered Optical Fiber Refractive Index Glucose Sensor

Erem Ujah
Old Dominion University, eujah001@odu.edu

ULTRASENSITIVE TAPERED OPTICAL FIBER REFRACTIVE INDEX GLUCOSE SENSOR

by

Erem Ujah
B.S. May 2022, North Carolina State University

A Thesis Submitted to the Faculty of
Old Dominion University in Partial Fulfillment of the
Requirement for the Degree of

MASTER OF SCIENCE

BIOMEDICAL ENGINEERING

OLD DOMINION UNIVERSITY
August 2023

Approved by:

Gymama Slaughter (Chair)

Nancy Xu (Member)

Barbara Hargrave (Member)

ABSTRACT

ULTRASENSITIVE TAPERED OPTICAL FIBER REFRACTIVE INDEX GLUCOSE SENSOR

Erem Ujah
Old Dominion University, 2023
Chair: Dr. Gymama Slaughter

Refractive index (RI) sensors are of great interest for label-free optical biosensing. A tapered optical fiber (TOF) RI sensor with micron-sized waist diameters can dramatically enhance sensor sensitivity by reducing the mode volume over a long distance. Here, a simple and fast method is used to fabricate extremely sensitive refractive index sensors based on localized surface plasmon resonance (LSPR). Two TOFs (l = 5 mm) with waist diameters of 5 μm and 12 μm demonstrated sensitivity enhancement at λ = 1559 nm for glucose sensing (5–45 wt%) at room temperature. The optical power transmission decreased with increasing glucose concentration due to the interaction of the propagating light in the evanescent field with glucose. The coating of the TOF with gold nanoparticles (AuNPs) as an active layer for glucose sensing generated LSPR through the interaction of the evanescent wave with AuNPs deposited at the tapered waist. The results indicated that the TOF (Ø = 5 μm) exhibited improved sensing performance with a sensitivity of 1265%/RIU compared to the TOF (Ø = 12 μm) at 560%/RIU towards glucose. The AuNPs were characterized using scanning electron microscopy and ultraviolent-visible spectroscopy. The AuNPs-decorated TOF (Ø = 12 μm) demonstrated a high sensitivity of 2032%/RIU toward glucose. The AuNPs- decorated TOF sensor showed a sensitivity enhancement of four times over TOF (Ø = 12 μm) with RI ranging from 1.328 to 1.393. The fabricated TOF enabled ultrasensitive glucose detection with good stability and fast response that may lead to next-generation ultrasensitive biosensors for real-world applications, such as disease diagnosis.

I dedicate this dissertation to my father, Ujah Olu, whose unwavering sacrifice and steadfast determination have instilled in me the belief that I can accomplish anything I set my heart and mind on. His enduring support has been the bedrock of my achievements. As well as my mother and siblings, who supported me throughout this process and believed in my ability to acquire my master's degree.

ACKNOWLEDGEMENTS

I am deeply grateful to my mentor, Dr. Gymama Slaughter, for her unwavering guidance throughout this journey. Her commitment to keeping me focused and aligned with my goals has been invaluable. Her grand expectations have constantly pushed me to deliver nothing short of my best. My heartfelt thanks to Dr. King, for guiding me through the writings process. Lastly, I would like to express my deep gratitude to Dr. Meimei Lai. Her teaching has laid a solid foundation for my understanding of this complex field, I appreciated how she took her time explaining concepts relate to optical research. Each of these individuals has played a significant role in my journey, and I am grateful for that.

Table of Contents

LIST OF TABLES

.

LIST OF FIGURES

CHAPTER 1

INTRODUCTION

Diabetes is a chronic disease that affects insulin production in the pancreas. Insulin is a hormone responsible for regulating the amount of glucose in the body. Defects in insulin production are characterized by type 1 and type 2 diabetes. In type 1 diabetes, the immune system attacks the beta cells in the pancreas that produce insulin. Individuals with type 1 diabetes must be administered insulin every day to survive. On the other hand, type 2 diabetes is known as insulin resistance, where the body either does not produce enough insulin or use it effectively resulting in less sugar intake into the cells. Measuring glucose levels accurately and in real-time is crucial for diabetes management.

This allows for the adjustment of treatment strategies and helps prevent the onset of severe complications, such as heart disease, kidney failure, and nerve damage.[1] Numerous methods exist for glucose detection, each presenting its own set of difficulties. Fingerstick Glucose Testing, a prevalent technique, can lead to discomfort due to the continual need for pricking one's finger. This method only offers a brief glimpse of the blood glucose level at the testing time, without indicating if the levels are rising or falling. The accuracy of this method hinges on the proper technique and can be swayed by factors like hydration, temperature, and altitude. Continuous Glucose Monitoring (CGM) provides a more comprehensive view of glucose levels but can be costly and isn't always covered by insurance.

The sensors need regular replacement, which can be bothersome. Some people may also have skin reactions to the adhesive used to attach the sensor. Moreover, CGM devices still requires calibration with fingerstick measurements. Hemoglobin A1C Testing gives a three-month average of glucose levels but doesn't provide daily data or capture daily fluctuations in blood glucose levels. The accuracy of this test can be influenced by certain conditions such as pregnancy, recent blood loss or transfusion, or certain types of anemia. The Oral Glucose Tolerance Test (OGTT) is time-intensive as it requires overnight fasting and multiple blood draws over several hours after consuming a glucose solution. It can also trigger side effects like nausea, sweating, or dizziness due to the high glucose intake.

The Fasting Plasma Glucose (FPG) Test, which requires an overnight fast, may not be convenient for all. Like the fingerstick test, it only offers a snapshot of glucose levels at a single point in time. The Random Plasma Glucose (RPG) Test doesn't require fasting, but it can be less accurate than other tests because glucose levels naturally fluctuate throughout the day. It's also less likely to identify prediabetes. Despite these challenges, these methods are vital for diabetes management. The choice of method often hinges on individual circumstances, including the type and severity of diabetes, lifestyle, and personal preferences.

Hence, continuous research investigates extremely sensitive biosensors capable of detecting minute changes in biological events. Biosensors detect biological events via interactions between analytes and biological components, converting bio-recognition interactions into measurable electrical signals generated through transducers, similar to analyte-bio-receptor interactions.[2] The mechanism of a biosensor comprises **(1)** an analyte, **(2)** a bio-receptor, **(3)** a transducer, **(4)** electronics, and **(5)** a display.[3]

1. **Analyte:** Target or molecule of interest (e.g., glucose, ammonia, alcohol, microRNA).
2. **Bioreceptor:** A biological element that binds to the target substrate.
3. **Transducer:** A device that converts energy to another form of energy (e.g., conversion of analyte-bio-recognition interaction into electric signal).
4. **Electronics:** The processing of the transducer signal.
5. **Display:** The display unit is based on the processed data.

Optics-based biosensors in glucose sensing have emerged as promising technological solutions due to their unique advantages. They offer high sensitivity, compactness and immunity to electromagnetic interference and have the potential for real-time monitoring. These characteristics make them particularly suitable for applications in biomedical sensing, where the need for accurate, reliable, and non-invasive sensors is paramount.[4] The operation of optical fiber sensors is based on the principle of light propagation, including the amplitude, phase velocity, and intensity of the transverse electromagnetic wave moving through the fiber. Changes in the surrounding environment alter these properties of the propagating light. This principle is exploited in the design of the ultrasensitive tapered optical fiber (TOF) refractive index glucose sensor.[5]

Besides TOFs sensors, there are various optical fiber-based glucose sensors, such as the U-shaped and Unclad sensors designed for sucrose detection, which are capable of detecting analytes with commendable sensitivity. However, they fall short regarding the ultra-sensitive detection capabilities exhibited by TOF bare fiber capability and amplification strategies. The superior detection capability of these latter sensors allows for a more accurate measurement of analytes,

which is crucial for non-invasive glucose management. The sensitivity of TOFs is enhanced due to the employment of the phenomenon known as Localized Surface Plasmonic Resonance (LSPR), which heightens its sensitivity by engaging with gold nanoparticles (AuNPs) and amplifying the evanescent field. This interaction prompts the electrons within the AuNPs to enter a state of excited state, oscillating, resulting in a standing wave. By coupling this oscillation with the photons in the evanescent field, the sensor can significantly prolong the interaction field with glucose molecules . The development of this sensor represents a significant advancement in glucose sensing technologies, which will significantly improve the quality of life for individuals living with diabetes and could have substantial implications for global health. The potential adaptation of these advanced sensors to detect other diseases, such as prostate cancer, is a promising avenue for future research and development.

1.1. Optical Biosensor

Optical biosensors fall into two main categories, label-free and label-based. Label-based sensing is particularly advantageous because it allows for an exceptionally low limit of detection (LOD) of the analyte, thanks to the sensitive capability based on the biosensor's sensitivity. However, there are drawbacks associated with label-based sensing, including the time-consuming nature of the labeling procedures. Additionally, these sensors are unable to provide real-time monitoring of analyte binding. This limitation is due to the requirement of additional reagents for labeled multiplex integration and analysis. Consequently, the use of multiple tags can introduce various inherent issues:

1. Short lifetime, excessive cost, and accumulation of hazardous contaminants involved in

radioisotope labeling.[6]

2. The use case of fluorophores, the excitation and emission efficiency are decreased by photo-bleaching and loss of kinetic information[7], causing uncertainty in data analysis.

Label-free optical biosensors are cost-effective and can perform real-time biosensing of analyte-biorecognition interactions, reducing detection uncertainty caused by label detection methodology. Furthermore, they offer a variety of configurations, with the most common fiber-based RI sensors being the Bragg grating (FBG) structures[8,9], long-period gratings (LPG) forming –Zehnder interferometer[10], micro interferometers[11] based on chemical etching and microstructure fibers[12] and taper optical fiber.[13]

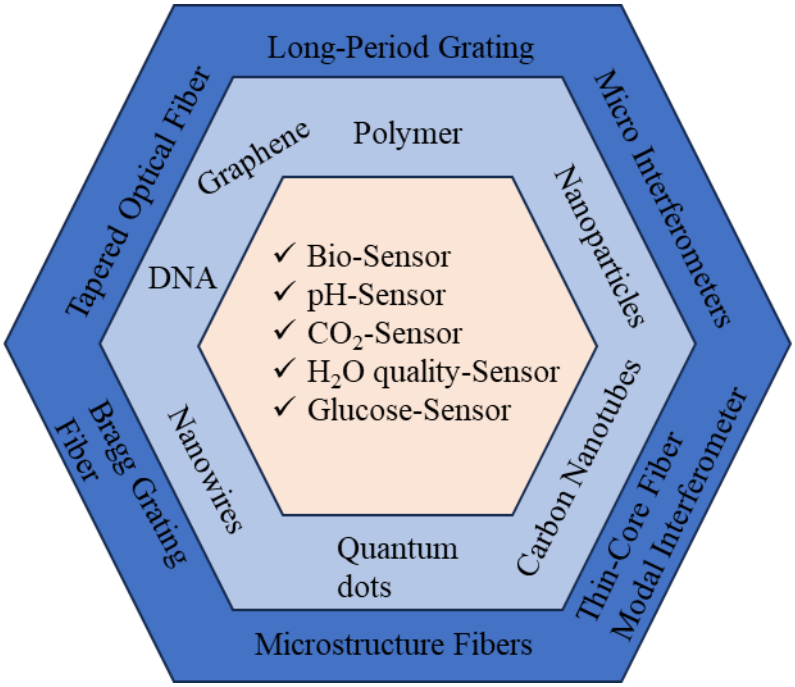

Figure 1. Fiber Optic-Based Configuration Application. Dark blue represents fiber optic design configuration; Light blue represents fiber coating for enhanced sensitivity and specificity; Light pink represents the sensing applications.

It is important to note that different combinations of nanomaterials with fiber optics configuration (Figure 1) and their concentrations will lead to different changes in the optical signal due the nanoparticle interaction with the evanescent wave. Selection of configuration determines ease of fabrication and coupling of light from the nanoparticle and evanescent wave increasing sensitivity of sensor. In addition to the attachment of a bio-recognition element such as DNA for selective binding to specific analyte, enabling the prediction of the analyte concentration through calibration acquiring specificity.

1.2. Evanescent Wave

When light is coupled into a material and strikes the interface between two non-absorbing structures with refractive indices n_i and refractive indices n_r (where $n_i > n_r$), a portion of the light is refracted while the remaining portion is reflected (Figure 2a). At the critical angle θ_c, the light propagates along the surface (Figure 2b) and the light is entirely reflected when the incident angle $\theta_i > \theta_c$ (Figure 2c). This phenomenon is known as total internal reflection (TIR), and the wave is referred to as a "guided wave."

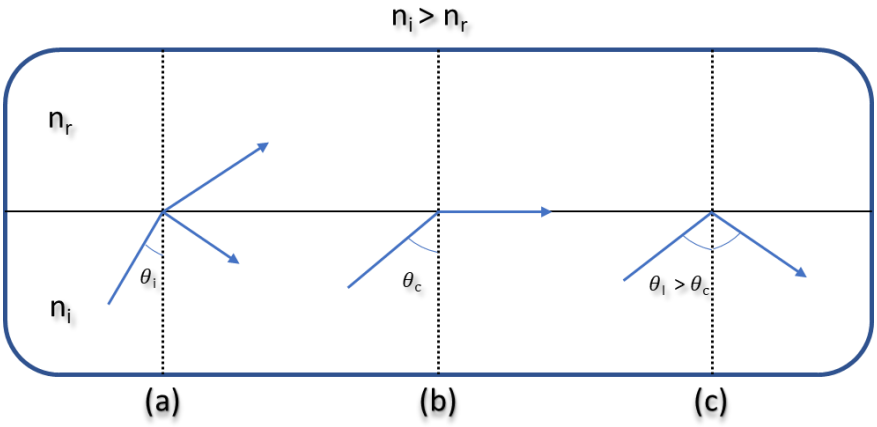

Figure 2. Total Internal Refection Principle. n_r and n_i are two different mediums in which light propagates, and the transition of one medium n_i to nr either shows that propagation changes. As the theta of the incident increases, so does the angle of reflection, which is shifted totally in n_i due to the theta critical angle in which the light is totally reflected inwards.

1.3. Tapered Optical Fiber (TOF)

Tapered optical fibers have emerged as a crucial tool in biosensing, owing to their distinctive characteristics and capacity for detecting even the subtlest changes. These fibers, crafted with a gradually diminishing diameter along their length (Figure 3), have

found considerable application, particularly in optical biosensing.[14]

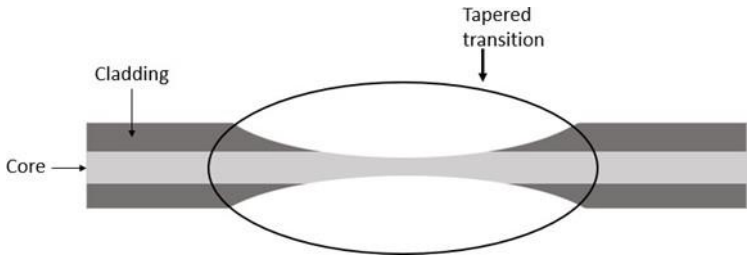

Figure 3. Optical Fiber Tapered Transition. Depiction of a tapered optical fiber tapered region.

The underlying principle governing the operation of tapered optical fiber sensors lies in the interaction between light and the encompassing medium. When light traverses the tapered section of the fiber, it engages with the surrounding medium, thereby inducing alterations in the transmitted light's properties. These alterations can be measured and linked to the properties of the encompassing medium, thereby facilitating the detection of specific substances or conditions.[15] One of the fundamental advantages bestowed upon tapered optical fiber sensors is their unparalleled sensitivity. This attribute arises from the intensified interaction between light and the surrounding medium within the tapered region, enabling the detection of infinitesimal changes in the medium's properties. A prime example encompasses using a biofunctionalized tapered optical fiber sensor blended with graphene oxide, successfully detecting Dengue virus E proteins with an astonishing detection limit of 1 pM.[2]

Furthermore, TOFs have been demonstrated to contain less than 100 photons at a time in the interaction (tapered) region using ultralow power level nonlinear spectroscopy. This low

radiation dose also reduces the risk of sample damage in the sensing environment. Another key advantage of using TOFs is their stability over time and self-cleaning capability via fluid motion.[16] TOF systems have been reported for biochemical sensing.[8, 17, 18, 19, 20, 21, 22] Moreover, tapered optical fiber sensors exhibit remarkable versatility. They can be enhanced by functionalizing various materials to heighten their sensing capabilities. For instance, a tapered optical fiber sensor was meticulously engineered to identify ascorbic acid - a biomarker for severe disorders. This sensor was fortified with gold and zinc oxide nanoparticles, augmenting sensitivity and selectivity.[3] To sum up, tapered optical fiber sensors hold tremendous potential for creating extremely sensitive and versatile biosensors. With their exceptional qualities and the opportunity for material functionalization, these sensors have power within the realm of biosensing.

1.4. Surface Plasmonic Resonance (SPR)

Surface Plasmon Resonance (SPR) has gained significant attention in the past few decades as a powerful label-free biosensing technique. SPR enables real-time, label-free detection of molecular interactions in various fields, including medical diagnostics, food safety, and environmental monitoring.[14] SPR is based on the interaction of light with a thin metal film, typically gold or silver, resulting in the collective oscillation of conduction electrons in the metal known as surface plasmons.[15] The surface plasmons are excited at a specific angle of incident light, known as the resonance angle, and the angle of reflected light changes in response to changes in the refractive index at the metal surface. SPR is extremely sensitive, with detection limits in the picomolar to femtomolar range.[2] Additionally, SPR is label-free, eliminating the need for fluorescent or radioactive labeling, which can interfere with the binding process.

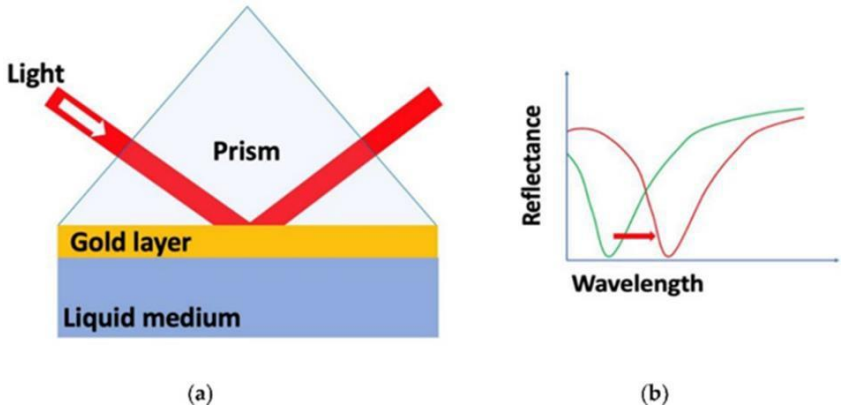

Figure 4. The Kretschmann Configuration. **(A)** Surface plasmon resonance biosensor based on the attenuated total reflection (ATR) method and **(B)** spectrum shifts observed before and after a change in the refractive index as the result of a biorecognition event.

One of the main advantages of SPR is its ability to detect molecular interactions in real-time, allowing for the study of binding kinetics and thermodynamics. The SPR technique has been used in various applications, including the detection of protein-protein interactions, DNA hybridization, small molecule-protein interactions, and virus detection.[3] Recently, there has been increasing interest in using SPR for the detection of cancer biomarkers, such as prostate-specific antigen (PSA), in blood serum. Several types of SPR configurations have been developed, including Kretschmann configuration, Otto configuration, and grating-coupled configuration.[14] The Kretschmann configuration illustrated in Figure 4 is the most widely used SPR configuration and consists of a thin metal film, typically gold or silver, deposited on a prism. The sample is introduced on the metal surface, and the binding of the analyte to the immobilized probe molecules on the surface causes a change in the refractive index, leading to a shift in the resonance angle.

The shift is measured by monitoring the intensity of the reflected light as a function of the incident angle.

1.5 Thesis Statement

This thesis explores developing and optimizing an ultrasensitive tapered optical fiber (TOF) sensor for glucose detection. Leveraging the unique properties of TOFs, such as their long interaction length and high intensity, we aim to enhance the light-matter interaction and thereby increase the sensor's sensitivity. We focused on the flame-brushing method for fabricating TOFs. The simplicity of the TOF fabrication method, setup cost, and ease of use make it effective in producing ultrasensitive TOFs for glucose detection. This thesis will delve into the intricacies of this method, exploring ways to optimize the process for better results. This thesis will also investigate the performance of the TOF sensor in glucose detection. Through rigorous testing and analysis, we aim to understand how the unique properties of TOFs can be leveraged to achieve high sensitivity.

The goal is to demonstrate that the TOF sensor can provide reliable and accurate glucose readings. Beyond glucose detection, the principles and techniques explored in this research could potentially be applied to detect various diseases such as breast, lung, and prostate cancer. This thesis aims to contribute to developing an extremely sensitive, cost-effective, and efficient glucose biosensor using TOFs. We believe that this research will not only have significant implications for diabetes management but also pave the way for advancements in various other fields through the application of TOF sensors. This opens new possibilities in environmental monitoring, industrial process control, and biomedical research.

CHAPTER 2

EXPERIMENTAL

2.1. Fabrication Of Tapered Optical Fiber

The flame brushing technique is the most used method for fabricating TOFs (Table 1). This straightforward and cost-effective method involves heating a glass optical fiber, with its cladding removed, at the center while simultaneously stretching it at both ends. This process results in a symmetrical "waist" formation in the fiber, making it a preferred choice for fabricating TOFs.

Table 1. Tapered Optical Fiber Fabrication Methods.

Fabrication method	Advantages	Disadvantages	References
Flame brushing	A straightforward way and low cost	low-cost varying lengths and diameters; Lack of uniformity of applied heat rough surface and insertion loss	13
Laser processing	Submicron dimensions Smooth surfaces	Requires specialized equipment and Insertion loss	23
Electrical heating	No turbulence in comparison to flame brushing	Non-even heating distribution	23
Chemical etching	High-quality and highly reproducible	Precision in hydrofluoric acid: time ratio; Limited control over the shape	24

The TOF was fabricated by the heat and pull method.[25] Briefly, the fiber coating on the two ends and the middle part of a standard commercially available optical fiber (Thorlabs1060XP, Single Mode Optical Fiber, 980–1600 nm, Extra-High Performance, ∅125 µm Cladding, ∅5.8 µm core) was carefully removed and cleaned with acetone. A propane air mixing flame was placed under bare fiber, as depicted in Figure 5. The bare fiber ends were placed on fiber holders (Newport 125 µm Fibers, 561 Series) and pulled by two Aerotech Pro115SL linear stages controlled by

A3200 Controllers to attain a sensing length of 5 mm (about 0.2 in). The transmission of the fiber was simultaneously monitored while pulling. The fabricated TOF was mounted in a custom-made canyon-shaped Teflon jig, and the sensing region was cleaned with acetone, followed by ultrapure deionized (DI) water rinse [26]. The canyon holds the sensing liquid (total volume = 2 ml).

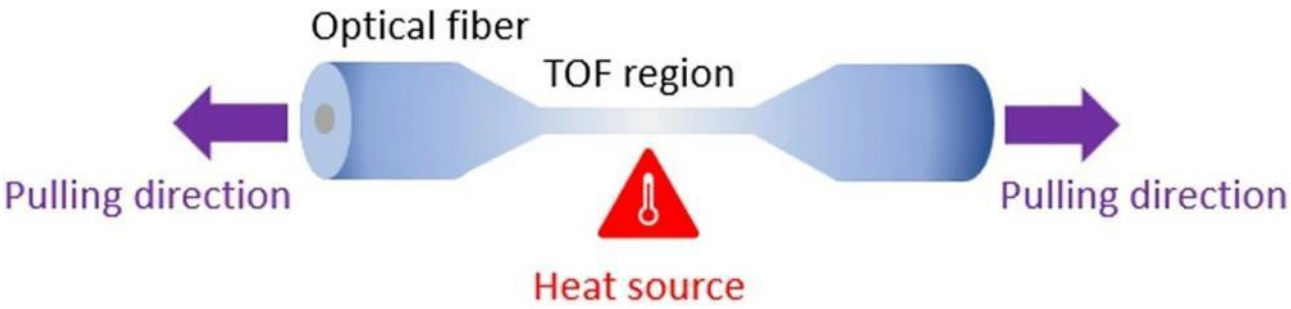

Figure 5. Tapered Optical Fiber Fabrication. Schematic illustration of the heat and pull method for creating tapered optical fiber.

2.2. Gold Nanoparticles Sythesis

As previously reported by Ma et al.[27], the gold nanoparticles were synthesized using a chemical method, as illustrated in Figure. 6. All glassware was cleaned with freshly prepared aqua regia (HCl: HNO_3, 3:1). The precursor solution was prepared using 0.01 g of gold (III) chloride trihydrate ($HAuCl_4 \cdot 3H_2O$) dissolved in 100 mL DI water (18.2 MΩ cm) and brought to a boil under constant stirring with a magnetic stirrer on a hot plate. Immediately following boiling, 3.2 mL 1 wt% of trisodium citrate ($Na_3C_6H_5O_7$) solution was quickly added and stirred for 10 min. The $Na_3C_6H_5O_7$ serves as the reducing and capping agent in nanoparticle synthesis. The solution's color changed from yellow to red wine during this period, signifying the fast reduction of gold.

The reaction solution was cooled to room temperature. The obtained AuNPs were centrifuged and resuspended in DI water and stored at 4 ºC when not in use. The UV–Vis spectra of AuNPs samples were recorded using UV–Vis absorption spectroscopy (Spectra Max M5 microplate reader, Molecular Devices, LLC.).

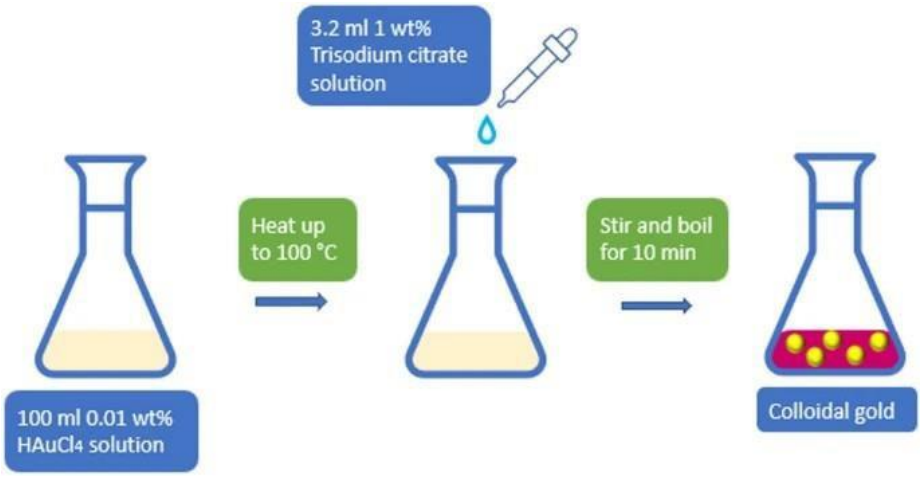

Figure 6. Gold Nanoparticles (AuNPs) Synthesis. Gold nanoparticle (AuNPs) synthesis by sodium citrate reduction method.

Afterward, the TOF fiber was functionalized by the salinization process method .[28] The sensing region of the TOF was cleaned with acetone, followed by a DI water rinse. After drying, the sensing region was immersed in freshly prepared piranha solution (H_2SO_4:H_2O_2, 3:1) for 30 min and thoroughly rinsed with DI water before drying at 90 for 30 min. Upon drying, the TOF was treated with a 1% (v/v) solution of 3-aminopropyltriethoxysilane (APTES) in ethanol for 24 hr at room temperature. The APTES functionalized TOF was rinsed with ethanol, followed by DI water rinse to remove any unbound APTES, and air dried. The functionalized TOF was incubated

in 2 mL of the synthesized AuNPs solution for 8 h at room temperature to form a coating of AuNPs on the TOF sensing region. The AuNPs-decorated TOF was rinsed with DI water and used for RI sensing. The use of organosilanes results in a very robust monolayer of metallic nanoparticles integration over the tapered optical fiber based on the chemisorption of nanoparticles.[29]

CHAPTER 3

RESULTS AND DISCUSSION

The experimental setup is shown in Figure 7. The TOF sensing region was suspended above the canyon floor and submerged entirely in the target analyte. The input light (Thorlabs ASE-FL7002 White Light Test Source, 1530–1610 nm) propagated through the TOF through an optical attenuator and polarization controllers. The light output was coupled to an Optical Spectrum Analyzer (Thorlabs OSA203C Fourier Transform Optical Spectrum).

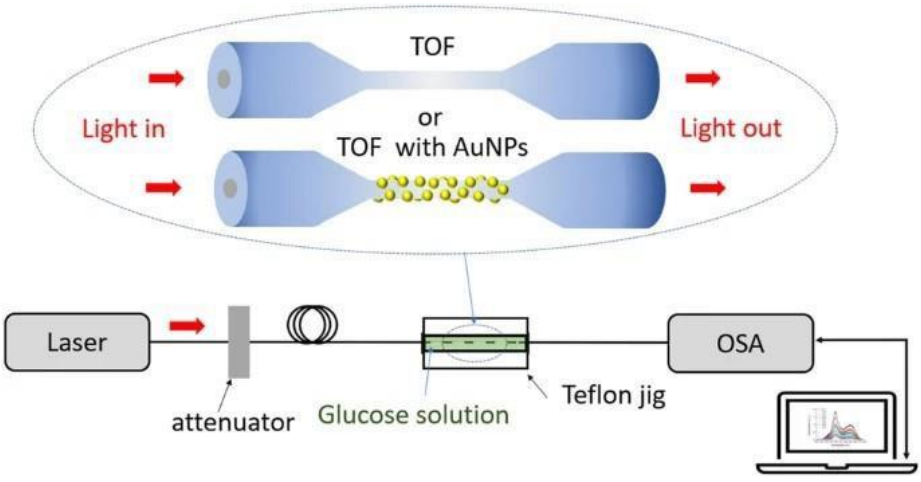

Figure 7. Experimental Setup for Glucose Sensing. Glucose RI sensing was conducted using a bare TOF and an AuNPs coated TOFs.

Analyzer, 1.0–2.6 µm). The TOF comprised a transition region with a smooth linear taper profile and a small uniform waist diameter (Ø=5 µm or Ø=12 µm). A series of aqueous glucose solutions

were prepared with mass ratios ranging from 0 to 45 wt%. The corresponding RI at 1559 nm was obtained.

3.1. Uv-Vis Spectroscopy And Structure Of Aunps

Figure 8A shows the UV–Vis absorption spectrum of the citrate-capped AuNPs in water. During the AuNPs synthesis, citrate reduces Au (III) to Au(0). The AuNPs exhibit a strong absorption peak at 524 nm. The absorbance peak suggests that AuNPs are approximately 24–33 nm in size and agrees with earlier reports.[30, 27, 31] Figure 8B shows the scanning electron microscopy (SEM) image of the bare TOF and AuNPs-decorated TOF RI sensor to confirm the chemisorption of AuNPs.

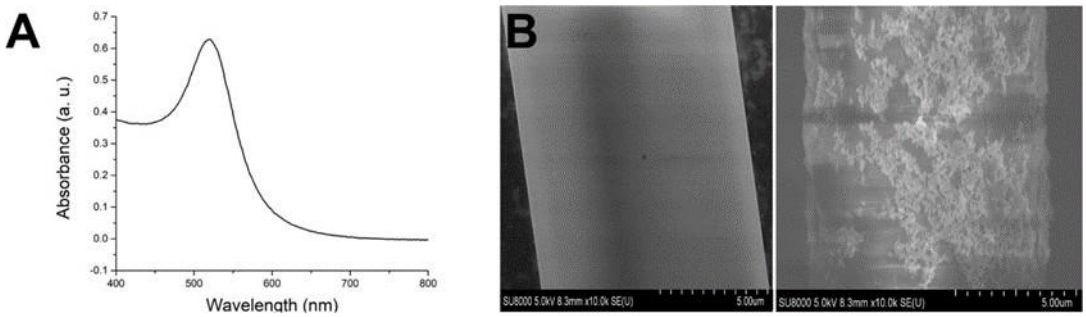

Figure 8. UV-Vis Spectra. **(A)** UV-Vis spectra of the synthesized gold nanoparticles (AuNPs). **(B)** Scanning electron microscopy (SEM) of bare and AuNPs-decorated TOF.

3.2. Localized Surface Plasmonic Resonance (LSPR)

Localized surface plasmon resonance (LSPR) is a label-free optical biosensor technology that uses metallic nanoparticles, typically gold or silver, that are functionalized with probes such as antibodies or aptamers.[3] When light is shone on the nanoparticles, the electrons in the metal

absorb the energy and oscillate, creating a plasmon resonance. When the nanoparticles are exposed to a sample containing target molecules, the plasmon resonance shifts due to changes in the local.

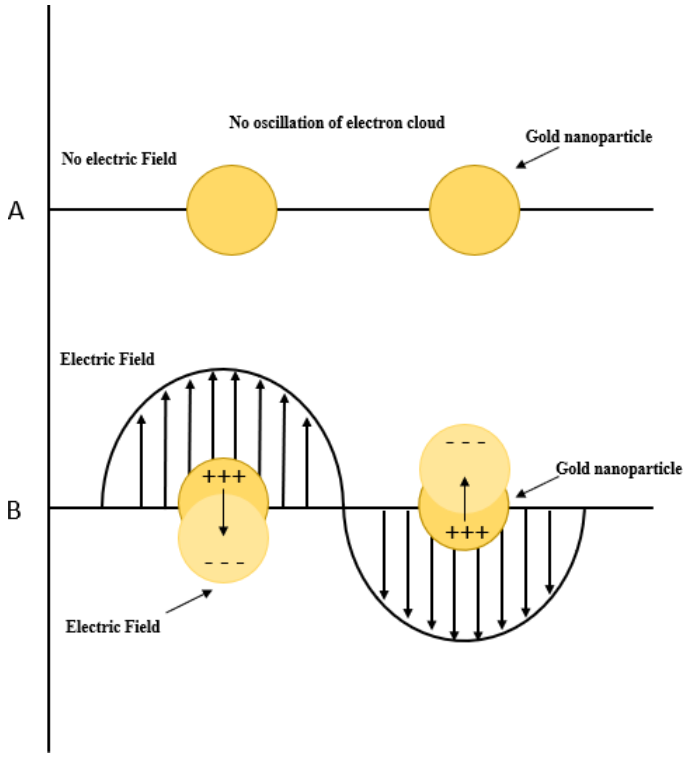

Figure 9. Localized Surface Plasmonic Resonance (LSPR). Illustration of gold nanoparticles oscillating in the electric field creating LSPR.

LSPR biosensors are based on the plasmonic properties of metallic nanoparticles, which are determined by the size, shape, and composition of the nanoparticles. The plasmonic properties of nanoparticles can be tuned by changing these parameters, allowing for the optimization of LSPR biosensors for specific applications.[3] Nano-spheres exhibit dipolar resonance with degenerated longitudinal and transverse modes due to spherical symmetry. The dipolar mode can be excited

when the incident light is polarized along the axis of the sphere, resulting in a strong absorption peak in the visible range of the electromagnetic spectrum. The dipolar mode is also known as the fundamental mode, and it is the most used plasmon resonance in LSPR biosensors.[3] In addition to the dipolar mode (Figure. 9), higher-order modes, such as quadrupolar, octupolar, and hexadecapolar modes, can also occur in metallic nanoparticles.[32]

These modes result from the multiple oscillations of the conduction electrons in the metal, giving rise to multipolar resonance. Multipolar resonance can increase the polarizability of the nanoparticles, leading to stronger plasmon resonances and higher sensitivity in LSPR biosensors.[3,32] In nanostructures with more than one nanoparticle, such as dimers or trimers, plasmon hybridization can occur, forming bonding and anti-bonding modes. The bonding mode is formed by symmetrical coupling in a nanostructure, resulting in a red shift in the plasmon resonance. The anti-bonding mode results from asymmetrical coupling in a nanostructure, resulting in a blue shift in the plasmon resonance.[3] In addition, plasmon hybridization can occur in nanostructures with more than one nanoparticle, forming bonding and anti-bonding modes.

These modes allow for the optimization of LSPR biosensors for specific applications by tuning the size, shape, and composition of the nanoparticles.

The functionalization of nanoparticles on TOFs has been reported to enhance the fiber optic-based RI sensor's properties by creating localized surface plasmonic resonance (LSPR).[33] Several types of nanoparticles, such as gold and silver,[34,35] magnetic nanoparticles, [36] [37,38] carbon-based nanoparticles[39,40] latex nanoparticles[41] and liposome-based nanoparticles have been used to enhance the surface plasmonic resonance signal for target analyte detection. AuNPs are widely used for functionalizing TOFs due to their strong induction of surface plasmonic resonance and

biocompatibility. Additionally, AuNPs are stable and resistant to oxidation, making them more durable for long-term applications.[22] demonstrated a localized sur- face resonance TOF sensor using AuNPs.

They achieved a waist diameter of 48 µm and a length of 1.25 mm and decorated it with AuNPs. A sensitivity of 380%/RIU with a refractive index ranging from 1.333 to 1.403 was reported.[42] Tai and Wei demonstrated an intensity sensitivity of up to 8000%/RIU using a tapered fiber tip to further enhance the sensitivity of optical fiber sensors due to the nanometer tip. Tapered fiber refractive index sensors exhibit excellent sensitivity with a fast response time to local changes in the refractive index in real time, which has enormous potential for label-free biosensing. The incorporation of LSPR and the optimized fabrication process of tapered optical fiber also enhances the detection calibration of biosensing, explored in this thesis through the RI detection of glucose, which has the potential for myriad biosensing for disease management and diagnosis.

3.3. Glucose Sensing

The comparative analysis of the optical spectra data indicates that the two TOFs with waist diameters of 5 µm (Figure 10A) and 12 µm (Figure 10B) impart the power output of the RI sensor. The power output response for the bare TOFs is observed across the near-infrared (NIR) wavelength range of 1520–1630 nm. Upon exposure to various glucose concentrations (5–45 wt%), the power output response decreases with the increase in glucose concentrations. The observed trend agrees with previous reports for other biomolecules.[27,30] The optical spectra were processed by integrating the area under the power output curve to generate the corresponding normalized power intensity curves depicted in Figure 10C,D.

At the peak wavelength of 1559 nm, the decrease in intensity can be clearly observed for each glucose concentration. No insignificant change was observed in the spectra after changing the light's polarization. This indicates that the TOF RI sensing is polarization insensitive, making it more practical.[31]

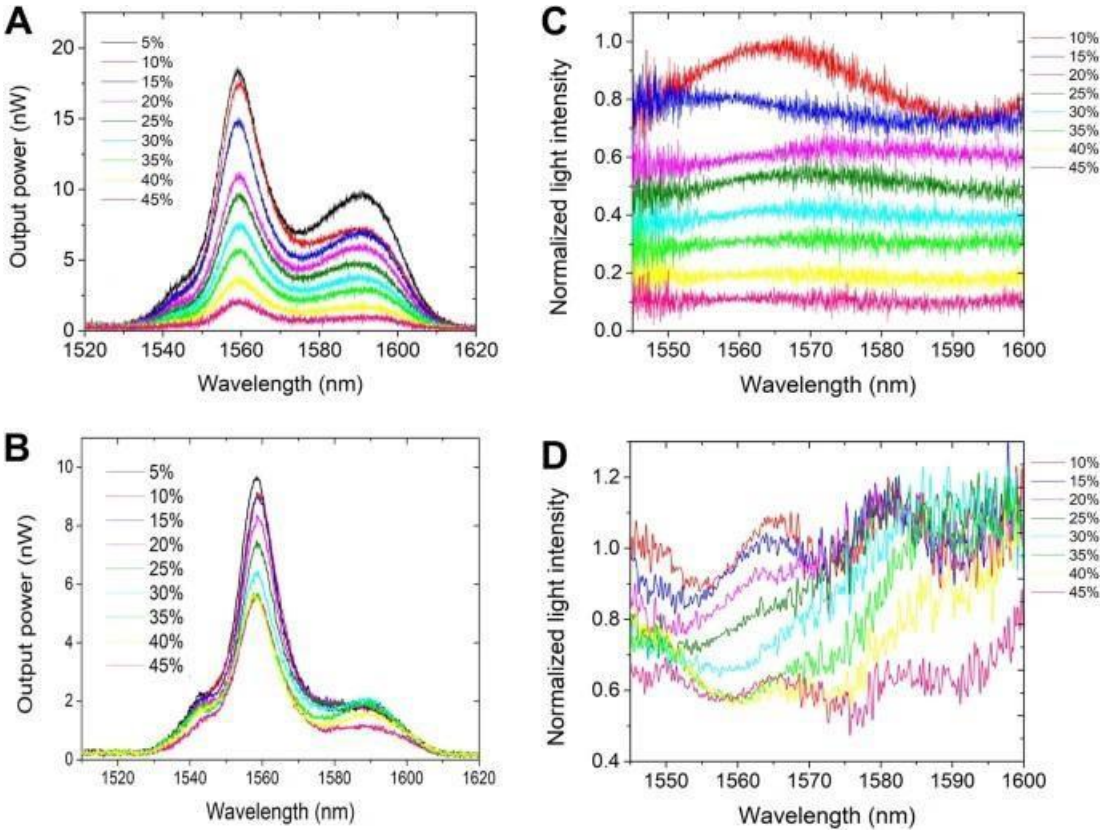

Figure 10. Bare TOF RI Glucose Sensing. Optical spectra of bare TOF sensors in different mass fractions of glucose solutions. **(A)** TOF (Ø = 5 µm diameter) and **(B)** TOF (Ø = 12 µm diameter). (C, D) Corresponding normalized intensity spectra.

The TOF with a larger waist diameter exhibited better reliability with reduced sensitivity. Therefore, to improve the sensitivity, AuNPs were coated on the surface of the fiber waist. From the AuNPs-decorated TOF (∅ = 12 µm) spectra (Figure 11A), it is observed that the sensor's

initial output in glucose is high due to the AuNPs coating. This is attributed to the inherently high sur- face area of the AuNPs and the LSPR, which enhance the interaction of glucose molecules with the sensing region, dramatically altering the evanescent field. The enhanced evanescent field penetration depth is modulated by the RI and enables a more intense power output than the bare TOFs. As the RI decreases, the surface evanescent wave penetration depth decreases, resulting in little interaction between the evanescent field and the glucose molecules and little power output in the detection spectrum. The corresponding normalized power intensity curves in Figure 11B shows that the AuNPs coating significantly enhances the sensitivity of the TOF RI sensor and further depicts the occurrence of glucose molecule interaction with the sensing region. Figure 12 shows the calibration curve for the bare TOF and the AuNPs-decorated.

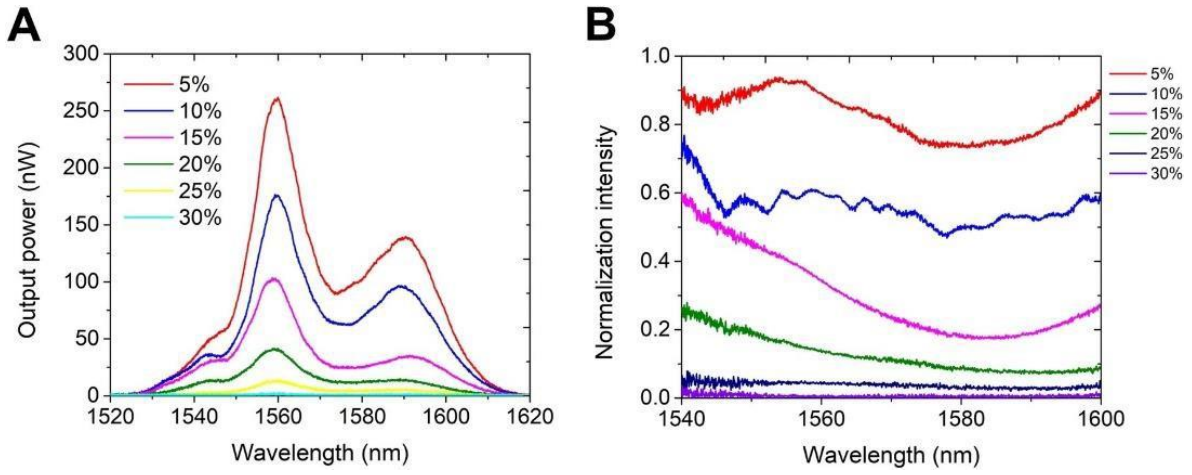

Figure 11. LSPR TOF RI Glucose Sensing. (**A**) Optical spectra of AuNPs decorated TOF (Ø = 12 µm diameter) sensor in different mass fractions of glucose solutions and **(B)** Corresponding normalized intensity spectra.

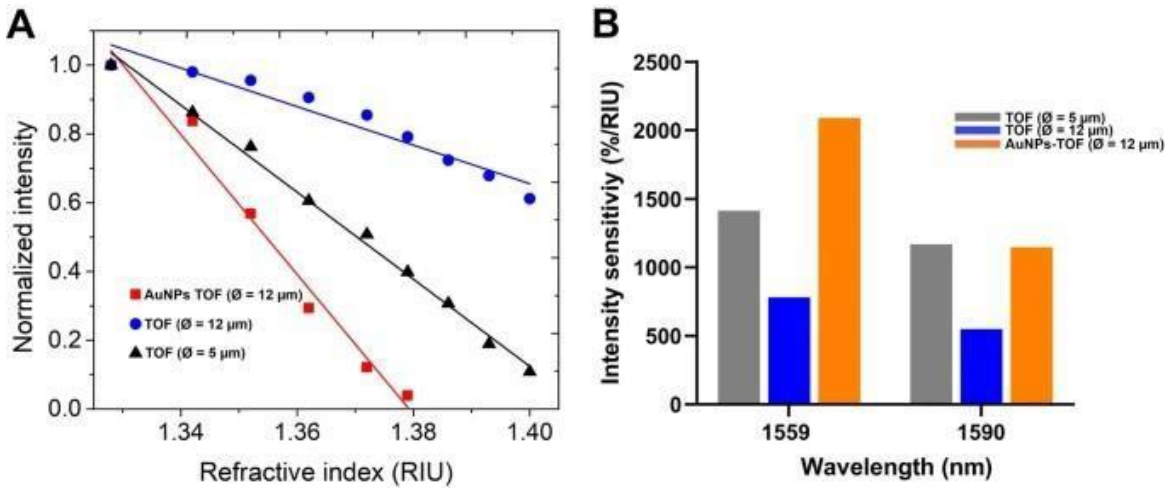

Figure 12. TOF Glucose Detection Comparison. (**A**) Power intensity changes against a refractive index of bare TOFs (red and blue), and AuNPs decorated TOF at λ = 1559 nm. (**B**) Comparison of the sensitivity of TOF RI sensors.

$$S = (\Delta I \,/\, I0)/\Delta n \cdot 100(\%/RIU) \quad (1)$$

A sensitivity of 2032% RIU at λ = 1559 nm was observed for the AuNPs-decorated TOF (Figure 12A), representing an increase by a factor of ~ 4 compared to the bare TOF. The AuNPs generate an LSPR signal with high sensitivity to detect slight changes in the reaction. However, the AuNPs-decorated TOF sensor saturated at 30 wt% glucose, wherein the peak at 1559 nm disappears. This may result from glucose molecules adsorbing onto the sensing region. Overall, the AuNPs-decorated TOF generated considerable power output changes than bare TOF. The sensitivity enhancement spans a broad-spectrum range (1540–1610 nm) and is uniform. Additionally, the optical performance of the as-fabricated TOF sensor was compared with other optical fiber-based RI sensors tested in various analytes, as summarized in Table 2.

Table 2. Comparison of the analyte characteristic of optical fiber RI sensors.

Fiber type	Analyte	Material	Sensitivity	Linear range	Wavelength	Reference
TOF tip	Glycerin	Bare	8000%/RIU	1.3-1.4	630nm	[42]
Coreless silica fiber	Glucose	Bare	1467.59nm/RIU	1.364 -1.397	1550 nm	[43]
Heterocore	NaCl	Mxene	510.1%/ RIU	1.3343–1.3765	500–1000 nm	[33]
Heterocore	NaCl	Bare	57.2%/RIU	1.3343–1.3765	500–1000 nm	[33]
U shape	Glucose	AuNPs Glucose oxidase	2.899 nm/%; 5.101 dB/%	0.1–0.5%	1400–1600 nm	[25]
Unclad fiber	Sucrose	AuNPs goat anti-rabbit IgG	13.09 AU/RIU	1.34–1.41	300–1000 nm	[31]
Tapered Optical Fiber	Glucose	Bare	1265%/RIU	1.328–1.393	1530–1610 nm	This work[44]
Tapered Optical Fiber	Glucose	AuNPs	2032%/RIU	1.328–1.379	1530–1610 nm	This work[44]

As the measured RI changed from 1.32 to 1.40, the change in light intensity was more significant, showing that the AuNPs can produce sensitivity enhancement for TOF RI sensors. AuNPs also enable more contact areas for glucose molecules to interact at the sensor surface. A linear RI range of 1.34–1.40 (r^2 = 0.9254) was observed for the TOF (⌀ = 12 µm), and a wider linear range of 1.32–1.40 (r^2 = 0.9940) was observed for the TOF (⌀ = 5 µm). A similar linear range of 1.328–1.393 (r^2 = 0.9781) was observed for the AuNPs decorated TOF and agrees with recently reported fiber optic RI sensors.[22,33] A heterocore fiber exhibited an intensity sensitivity of 57.2%/RIU within a range of 1.334–1.377, and an MXene nanosheet-based hetero- core fiber demonstrated a sensitivity of 510.1%/RIU with a range of 1.334–1.377.[33] Therefore, the AuNPs-decorated TOF RI sensor enhances the evanescent field to detect the RI change in the sensing

environment, making the sensor ideal for glucose detection. Figure 12B compares the TOF RI sensor's sensitivity at 1559 nm and 1590 nm. These uniform sensitivities indicate that the AuNPs-decorated TOF RI sensor is a good option for biochemical detection at 1559 nm and 1590 nm.

CHAPTER 4

CONCLUSION AND FUTURE WORK

In summary, we described and demonstrated the use of TOF as RI sensors for detecting various glucose concentrations. As the glucose concentration increased from 5 to 45 wt%, the sensor's power output intensity decreased consequently. Additionally, the bare TOF's sensitivity is highly related to its diameter and insensitive to light polarization, which is ideal for real-world applications. The bare TOF (⌀ = 5 µm) sensor demonstrated better sensing capabilities than the bare TOF (⌀ = 12 µm). We achieved an intensity sensitivity of 1265%/RIU over the RI range of 1.328–1.393.

Upon decorating the TOF (⌀ = 12 µm) with AuNPs, the sensor's sensitivity increased by ~ 4 times, although the linear RI range decreased slightly. The sensitivity was 2032%/RIU over the RI range of 1.328–1.379. The smaller the waist diameter TOF, the more sensitive the sensor was to changes in the biochemical environment. And the AuNPs decoration on the TOF surface resulted in sensitivity enhancement due to the high surface-to-volume ratio enabled by the AuNPs for biomolecule adsorption and the generation of localized surface plasmon resonance. The TOF (⌀ = 12 µm) preparation method is simple, robust, reproducible, and can easily be decorated with nanomaterials to enhance sensing capability. However, the micron-sized tapered fiber sensor is exceptionally fragile, and its mechanical strength will need to be improved for real-world applications. Future research will focus on enhancing the selectivity and specificity of tapered

optical fibers by leveraging the bio-recognition capabilities of the surface of the TOF. This approach aims to achieve more accurate detection of target analytes. In addition, we will explore novel methods to increase the integrity of the fiber, such as functionalizing nanotubes with gold nanoparticles on the TOF.[45] To fully realize the potential of these advancements, we plan to incorporate large-scale integration of multiplexing in an optical system with microfluidic implementation.[32] This integration will pave the way for miniaturized devices capable of simultaneous multi-detection of analytes, thanks to the benefits of microfluidic integration. Furthermore, integrating the sensor into wearable devices for convenient and continuous glucose monitoring.

REFERENCES

1 Zhong, N. *et al.* Temperature-independent polymer optical fiber evanescent wave sensor. *Scientific Reports* (2015). https://doi.org:https://dx.doi.org/10.1038/srep11508

2 Kulkarni, M., Ayachit, N. & Aminabhavi, T. Biosensors and microfluidic biosensors: From fabrication to application. *Biosensors* **12**, 543 (2022).

3 Vazan, M. Introduction to biosensors. (2019).

4 Novais, S., Ferreira, C. I. A., Ferreira, M. S. & Pinto, J. L. Optical fiber tip sensor for the measurement of glucose aqueous solutions. *IEEE Photonics Journal* **10**, 1--9 (2018).

5 Kim, J., Son, C., Choi, S., Yoon, W. J. & Ju, H. A Plasmonic Fiber Based Glucometer and Its Temperature Dependence. *Micromachines* (2018). https://doi.org:https://dx.doi.org/10.3390/mi9100506

6 Mukherji, S. & Punjabi, N. Label—Free integrated optical biosensors for multiplexed analysis. *Journal of the Indian Institute of Science* **92**, 253--294 (2012).

7 Lakowicz, J. R. *Principles of Fluorescene Spectroscopy*. 17 April 2013 edn, (2013).

8 Hendrickson, S. M., Lai, M. M., Pittman, T. B. & Franson, J. D. Observation of two-photon absorption at low power levels using tapered optical fibers in rubidium vapor. *Physical review letters* **105**, 173602 (2010).

9 Ahlfeldt, A. A. S. S. H. & Edwall, B. S. R. S. G. Fiber optical Bragg grating refractometer. *Fiber \& Integrated Optics* **17**, 51--62 (1998).

10 Vengsarkar, A. M. *et al.* Long-period fiber gratings as band-rejection filters. *Journal of lightwave technology* **14**, 58--65 (1996).

11 Gong, Y., Guo, Y., Rao, Y.-J., Zhao, T. & Wu, Y. Fiber-optic Fabry--P \'e rot sensor based on periodic focusing effect of graded-index multimode fibers. *IEEE Photonics Technology Letters* **22**, 1708--1710 (2010).

12 Ran, Z. L., Rao, Y. J., Liu, W. J., Liao, X. & Chiang, K. S. Laser-micromachined Fabry-Perot optical fiber tip sensor for high-resolution temperature-independent measurement of refractive index. *Optics express* **16**, 2252--2263 (2008).

13 Zhu, G. *et al.* Tapered optical fiber-based LSPR biosensor for ascorbic acid detection. *Photonic Sensors* **11**, 418--434 (2021).

14 Lai, M. & Slaughter, G. Label-free microrna optical biosensors. *Nanomaterials* **9**, 1573 (2019).

15 Tazawa, H., Kanie, T. & Katayama, M. Fiber-optic coupler based refractive index sensor and its application to biosensing. *Applied Physics Letters* **91**, 113901 (2007).

16 Irigoyen, M., Snchez-Martin, J. A., Bernabeu, E. & Zamora, A. Tapered optical fiber sensor for chemical pollutants detection in seawater. *Measurement Science and Technology* **28**, 045802 (2017).

17 Korposh, S., James, S. W., Lee, S.-W. & Tatam, R. P. Tapered optical fibre sensors: Current trends and future perspectives. *Sensors* **19**, 2294 (2019).

18 Kim, H.-M., Park, J.-H. & Lee, S.-K. Fiber optic sensor based on ZnO nanowires decorated by Au nanoparticles for improved plasmonic biosensor. *Scientific Reports* **9**, 1--9 (2019).

19 Wieduwilt, T. *et al.* Gold-reinforced silver nanoprisms on optical fiber tapers—A new base for high precision sensing. *Apl Photonics* **1**, 066102 (2016).

20 Kumar, S. *et al.* LSPR-based cholesterol biosensor using a tapered optical fiber structure. *Biomedical Optics Express* **10**, 2150--2160 (2019).

21 Rodríguez-Schwendtner, E., González-Cano, A., Díaz-Herrera, N., Navarrete, M. C. & Esteban, Ó. Signal processing in SPR fiber sensors: Some remarks and a new method. *Sensors and Actuators B: Chemical* **268**, 150-156 (2018). https://doi.org:https://doi.org/10.1016/j.snb.2018.04.083

22 Lin, H.-Y., Huang, C.-H., Cheng, G.-L., Chen, N.-K. & Chui, H.-C. Tapered optical fiber sensor based on localized surface plasmon resonance. *Optics Express* **20**, 21693--21701 (2012).

23 Brandon Johann, B. & Jonathan Clyde, S. (2017).

24 Zhang, E. J., Sacher, W. D. & Poon, J. K. S. Hydrofluoric acid flow etching of low-loss subwavelength-diameter biconical fiber tapers. *Optics Express* **18**, 22593--22598 (2010).

25 Chen, K.-C., Li, Y.-L., Wu, C.-W. & Chiang, C.-C. Glucose sensor using U-shaped optical fiber probe with gold nanoparticles and glucose oxidase. *Sensors* **18**, 1217 (2018).

26 Liyanage, T., Alharbi, B., Quan, L., Esquela-Kerscher, A. & Slaughter, G. Plasmonic-based biosensor for the early diagnosis of prostate cancer. *ACS omega* **7**, 2411--2418 (2022).

27 Haiss, W., Thanh, N. T. K., Aveyard, J. & Fernig, D. G. Determination of size and concentration of gold nanoparticles from UV- Vis spectra. *Analytical chemistry* **79**, 4215--4221 (2007).

28 Kyaw, H. H., Al-Harthi, S. H., Sellai, A. & Dutta, J. Self-organization of gold nanoparticles on silanated surfaces. *Beilstein journal of nanotechnology* **6**, 2345--2353 (2015).

29 Pisco, M. & Cusano, A. Lab-on-fiber technology: a roadmap toward multifunctional plug and play platforms. *Sensors* **20**, 4705 (2020).

30 Ma, Y. *et al.* Colorimetric sensing strategy for mercury (II) and melamine utilizing cysteamine-modified gold nanoparticles. *Analyst* **138**, 5338--5343 (2013).

31 Shen, Z. & Du, M. High-performance refractive index sensing system based on multiple Fano resonances in polarization-insensitive metasurface with nanorings. *Optics Express* **29**, 28287--28296 (2021).

32 Sui, M., Kunwar, S., Pandey, P., Pandit, S. & Lee, J. Improved localized surface plasmon resonance responses of multi-metallic Ag/Pt/Au/Pd nanostructures: systematic study on the fabrication mechanism and localized surface plasmon resonance properties by solid-state dewetting. *New Journal of Physics* (2019). https://doi.org:10.1088/1367-2630/ab5694

33 Chen, C. & Wang, J. Optical biosensors: an exhaustive and comprehensive review. *Analyst* **145**, 1605-1628 (2020). https://doi.org:10.1039/c9an01998g

34 Cano Perez, J. L. *et al.* Fiber optic sensors: a review for glucose measurement. *Biosensors* **11**, 61 (2021).

35 Cathcart, N., Chen, J. I. L. & Kitaev, V. LSPR tuning from 470 to 800 nm and improved stability of Au--Ag nanoparticles formed by gold deposition and rebuilding in the presence of poly (styrenesulfonate). *Langmuir* **34**, 612--621 (2018).

36 Hobbs, K., Cathcart, N. & Kitaev, V. Gold-plated silver nanoparticles engineered for sensitive plasmonic detection amplified by morphological changes. *Chemical Communications* **52**, 9785--9788 (2016).

37 Jia, Y. *et al.* Magnetic nanoparticle enhanced surface plasmon resonance sensor for estradiol analysis. *Sensors and Actuators B: Chemical* **254**, 629--635 (2018).

38 Liu, X. *et al.* Surface plasmon resonance immunosensor for fast, highly sensitive, and in situ detection of the magnetic nanoparticles-enriched Salmonella enteritidis. *Sensors and Actuators B: Chemical* **230**, 191--198 (2016).

39 Lee, E. G. *et al.* Carbon nanotube-assisted enhancement of surface plasmon resonance signal. *Analytical biochemistry* **408**, 206--211 (2011).

40 Zhang, H. *et al.* A novel graphene oxide-based surface plasmon resonance biosensor for immunoassay. *Small* **9**, 2537--2540 (2013).

41 Severs, A. H. & Schasfoort, R. B. M. Enhanced surface plasmon resonance inhibition test (ESPRIT) using latex particles. *Biosensors and Bioelectronics* **8**, 365--370 (1993).

42 Tai, Y.-H. & Wei, P.-K. Sensitive liquid refractive index sensors using tapered optical fiber tips. *Optics letters* **35**, 944--946 (2010).

43 Novais, S., Ferreira, C. I. A., Ferreira, M. & Pinto, J. Optical Fiber Tip Sensor for the Measurement of Glucose Aqueous Solutions. *IEEE Photonics Journal* (2018). https://doi.org:https://dx.doi.org/10.1109/JPHOT.2018.2869944

44 Ujah, E., Lai, M. & Slaughter, G. Ultrasensitive tapered optical fiber refractive index glucose sensor. *Scientific Reports* **13**, 4495 (2023).

45 Ding, Z. *et al.* A Mass-Producible and Versatile Sensing System: Localized Surface Plasmon Resonance Excited by Individual Waveguide Modes. *ACS Sensors* (2018). https://doi.org:10.1021/acssensors.7b00736

VITA

Erem Ujah
Department of computer science and electrical engineering
Old Dominion University
Norfolk, VA 23529

EDUCATION

B.S. (May 2023) in physics, North Carolina Central University, Durham, NC 27707

PROFESSIONAL EXPERIENCE

2020-2022, Neutrino physicist intern, Triangle University Nuclear Laboratories (TUNL), Duke University, North Carolina
2021-2021, Neutrino physicist intern, Oak Ridge National Laboratory (ORNL), Tennessee
2019-2019, UAV Engineer intern, North Carolina State University (NCSU), North Carolina

CONFERENCE PRESENTATIONS

U. Erem, WEEF & GEDC partnering with AEEA Conference, Ultra-sensitive optical biosensor for early detection for prostate cancer three-minute thesis presentation, November 2021
U. Erem, Southern Section of the American Physics Society, Characterization of Na [TI] Crystals for Ton-scale Detector Array, November 2021
U. Erem, Magnificent CEvNS workshop, Characterization of Na [TI] Crystals for Ton-scale Detector Array, November 2019
U. Erem, Southern Section of the American Physics Society, Characterization of Na[TI] Crystals for Ton-scale Detector Array, November 2019

PUBLICATIONS

E Ujah, M Lai, G Slaughter, Ultrasensitive tapered optical fiber refractive index glucose sensor, Scientific Reports, 13, 4495, 2023
M Lai, E Ujah, G Slaughter, Ultralow Power Refractive Index Tapered Optical Fiber Glucose Sensor, Optica Publishing Group, JW2B-3, 2023
D. Akimov, U. Erem, COHERENT TEAM, A DO_2 detector for flux normalization of a pion decay at-rest neutrino source, Journal of Instrumentation, Volume 16, August 2021